Electronic Supplementary Material (ESI) for Dalton Transactions.
This journal is © The Royal Society of Chemistry 2024

Radical and diradical states of bis(molybdenocene dithiolene) complexes

Khalil Youssef, Corentin Poidevin, Antoine Vacher, Arnaud Fihey, Yann Le Gal, Thierry Roisnel, Dominique Lorcy*

Univ Rennes, CNRS, ISCR (Institut des Sciences Chimiques de Rennes) - UMR 6226, F-35000 Rennes, France

Table of contents

Table S1 Intramolecular Bond lengths (in Å) in the following proligands: **2**, **3**, **4** and **5**.

Bonds 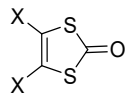	**2** X = S	**4** X = Si	**5** X = C	Bonds 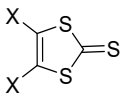	**3** X = Si
C—X	1.761(4)	1.874(2)	1.390(3)	C—X	1.883(3)
	1.765(4)	1.875(2)	1.390(4)		1.883(3)
C=C	1.336(6)	1.354(2)	1.397(4)	C=C	1.354(4)
C—S	1.745(4)	1.749(2)	1.747(3)	C—S	1.748(3)
	1.745(4)	1.751(2)	1.750(3)		1.744(3)
S—C	1.785(4)	1.769(2)	1.774(3)	S—C	1.728(3)
	1.780(4)	1.768(2)	1.778(3)		1.728(3)
C=O	1.211(5)	1.208(2)	1.200(3)	C=S	1.652(3)

If we compare the bond lengths of the proligands within the bisdithiole-2-one series, compounds **2**, **4** and **5**, besides the expected changes in the bond lengths of C—X (X = S, Si and C), the main difference is observed in the C=C bond, of the dithiole ring. Indeed, the shortest one is for the dithiine **2** and the longest for the aromatic ring of the benzo-fused **5**.

Table S2 Significant bond lengths (Å) and angles (°) of **Cp_2MoS_2** and **Cp_2MoS_2CO**

Bonds 	**Cp_2MoS_2**	Bonds 	**Cp_2MoS_2CO** **Mo1**	**Mo2**
		C=O	1.208(13)	1.206(17)
		C—S	1.761(11)	1.765(11)
S—S	2.055(3)			1.766(11)
S—Mo	2.459(2)	S—Mo	2.457(3)	2.454(3)
	2.455(3)		2.457(3)	2.458(3)
	49.4(1)		70.5(1)	70.6(1)

The **Cp_2MoS_2CO** crystallizes in the monoclinic system, space group *Cc* and the unit cell contains two crystallographically independent molecules, both in general position. The **Cp_2MoS_2** crystallizes in the orthorhombic system, space group $P2_12_12_1$ and the unit cell contains one crystallographically independent molecule in general position. The two **Cp_2MoS_2CO** complexes present similar bond lengths but the shape of the metallacycles MoS_2C is different as the one with Mo1 is slightly distorted along the S---S axis by 4.3(4)° and the one with Mo2 is planar. On the other hand, the S—Mo—S angle decreases significantly with the size of the metallacycle since it goes from 82.4° in the five membered ring of **Modt** to 70.6° in the four membered ring in **Cp_2MoS_2CO** to reach 49.4° in the 3 membered ring of **Cp_2MoS_2**.

Table S3 Crystallographic data of compounds **2**, **3**, **4** and **5**

	2	**3**	**4**	**5**
Formulae	$C_6O_2S_6$	$C_{10}H_{12}S_6Si_2$	$C_{10}H_{12}O_2S_4Si_2$	$C_8H_2O_2S_4$
FW (g.mol^{-1})	296.42	380.74	348.62	258.34
System	orthorhombic	monoclinic	monoclinic	monoclinic
Space group	*Fdd2*	*P2$_1$/c*	*P2$_1$/c*	*P2$_1$/c*
a (Å)	17.925(2)	6.6939(16)	6.9743(10)	3.8723(7)
b (Å)	26.902(3)	7.9864(19)	8.8737(11)	11.708(2)
c (Å)	3.9069(4)	15.384(4)	12.5077(14)	9.9274(17)
α (deg)	90	90	90	90
β (deg)	90	90.118(11)	94.939(6)	90.310(7)
γ (deg)	90	90	90	90
V (Å^3)	1884.0(4)	822.5(3)	771.20(17)	450.06(14)
T (K)	150(2)	150(2)	150(2)	150(2)
Z	8	2	2	2
D_{calc} (g.cm^{-3})	2.090	1.537	1.501	1.906
μ (mm^{-1})	1.412	0.957	0.761	1.016
Total refls	1909	3474	8227	3667
Abs corr	multi-scan	multi-scan	multi-scan	multi-scan
Uniq refls (R_{int})	1020 (0.0216)	1845 (0.0298)	1772 (0.0405)	1019 (0.0408)
Uniq refls (I > 2σ(I))	957	1374	1537	963
R_1, wR_2	0.0312, 0.0679	0.0407, 0.0843	0.0297, 0.0686	0.0344, 0.0826
R_1, wR_2 (all data)	0.0340, 0.0692	0.0626, 0.0946	0.0352, 0.0699	0.0376, 0.0846
GOF	1.056	0.981	1.134	1.017

Table S4 Crystallographic data mononuclear complexes

	Modt	**Cp_2MoS_2**	**Cp_2MoS_2CO**	**$MoSi_2$**
Formulae	$C_{12}H_{12}MoS_2$	$C_{10}H_{10}MoS_2$	$C_{11}H_{10}MoOS_2$	$C_{19}H_{22}MoOS_4Si_2$
FW (g.mol^{-1})	316.28	290.24	318.25	546.72
System	monoclinic	orthorhombic	monoclinic	monoclinic
Space group	*P2$_1$/n*	*P2$_1$2$_1$2$_1$*	*Cc*	*P2$_1$/c*
a (Å)	11.3393(11)	5.9374(4)	12.0971(13)	11.8373(13)
b (Å)	7.7186(7)	12.6972(7)	10.8907(12)	15.1681(15)
c (Å)	13.8396(13)	13.0938(7)	16.869(2)	12.7361(12)
α (deg)	90	90	90	90
β (deg)	114.361(3)	90	102.634(4)	103.610(4)
γ (deg)	90	90	90	90
V (Å^3)	1103.44(18)	987.12(10)	2168.6(4)	2222.5(4)
T (K)	150(2)	150(2)	150(2)	150(2)
Z	4	4	8	4
D_{calc} (g.cm^{-3})	1.904	1.953	1.949	1.634
μ (mm^{-1})	1.526	1.696	1.560	1.082
Total refls	16085	3770	8162	22053
Abs corr	multi-scan	multi-scan	multi-scan	multi-scan
Uniq refls (R_{int})	2509 (0.0498)	2131 (0.0235)	4096 (0.0331)	5089 (0.0371)
Uniq refls (I >	2348	1941	4051	4454

2σ(I))				
R_1, wR_2	0.0263, 0.0664	0.0432, 0.0900	0.0617, 0.1540	0.0453, 0.1224
R_1, wR_2 (all data)	0.0280, 0.0689	0.0483, 0.0935	0.0619, 0.1544	0.0521, 0.1299
GOF	1.048	0.993	1.081	1.006

Fig. S1 Top and side views of the molecular structure of compound **3**

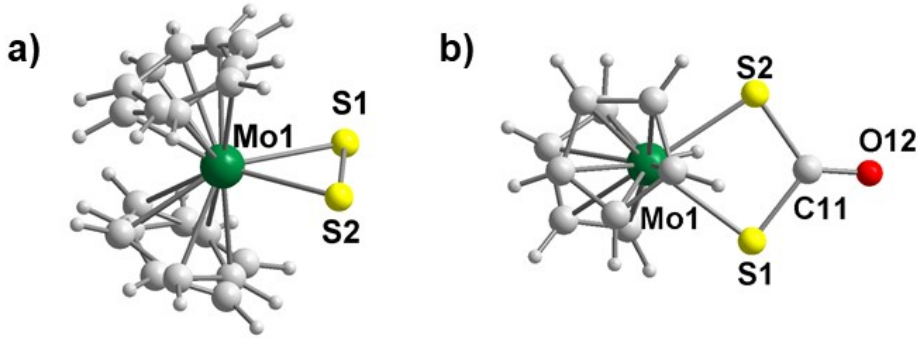

Fig. S2 Molecular structures of **Cp_2MoS_2** (a) and **Cp_2MoS_2CO** (b).

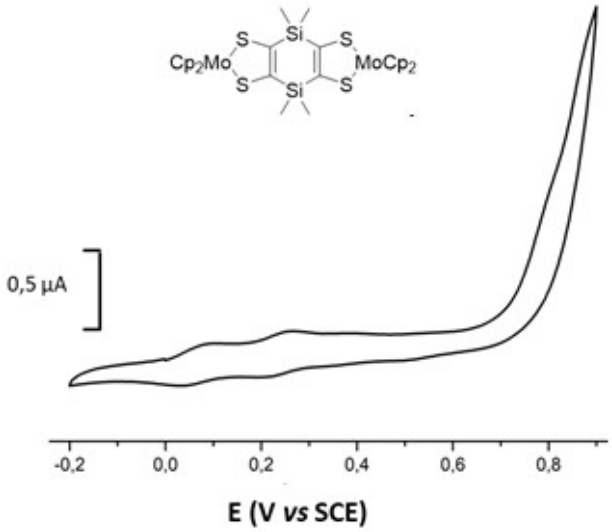

Fig. S3 Cyclic voltammogram of **Mo_2Si_2** in DMSO with Bu_4NPF_6 0.1 M (100 mV/s).

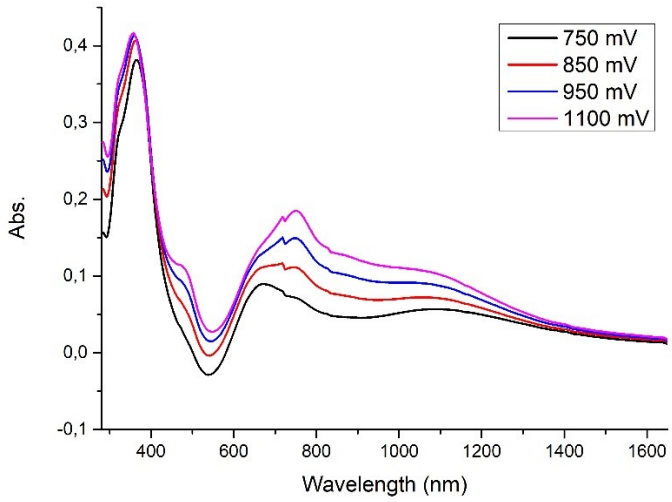

Fig. S4 Differential UV-vis-NIR absorption spectra of the **Modt** complex monitored from the monocation radical state to the dicationic state upon electrochemical oxidation in CH_2Cl_2-$[Bu_4N][PF_6]$

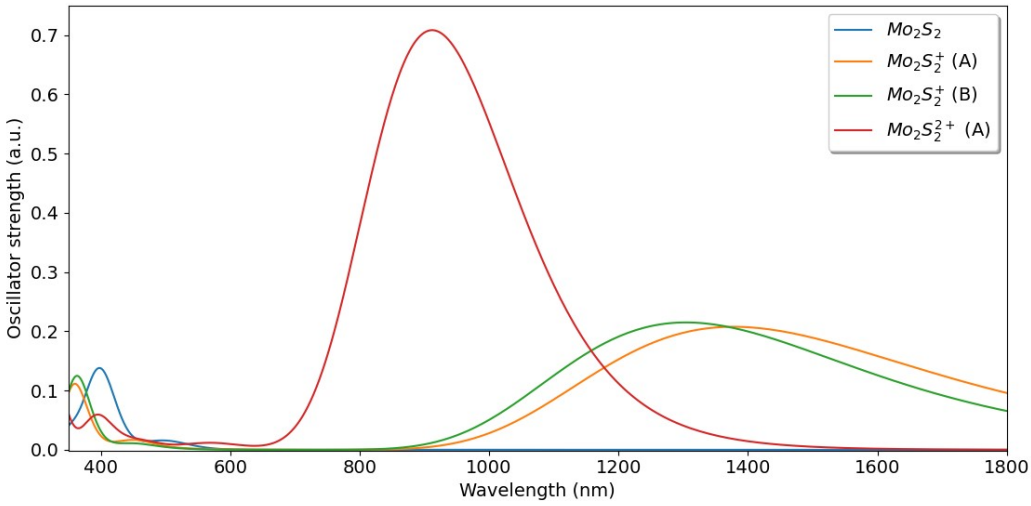

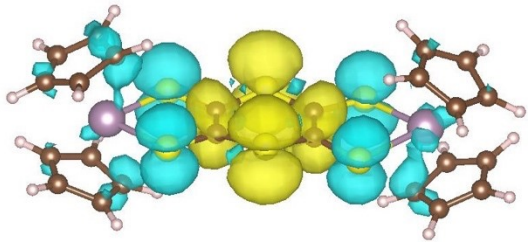

Fig. S5 Top: simulated UV-vis-NIR absorption spectra of $\mathbf{Mo_2S_2}$, $\mathbf{Mo_2S_2^{+\bullet}}$ and $\mathbf{Mo_2S_2^{2+}}$ computed at the CAM-B3LPY/def2-TZVP with CPCM(DMSO). Bottom: Characteristic charge density difference plots of the first excited state of $\mathbf{Mo_2S_2^{2+}}$ absorbing around 1000 nm.

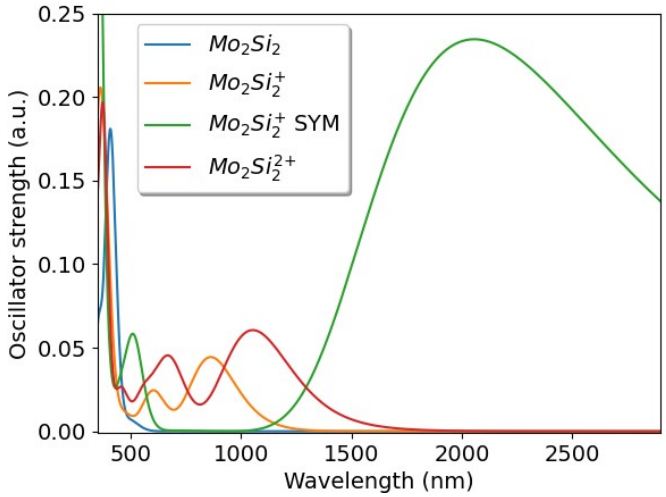

Fig. S6 UV-vis-NIR absorption spectra of $\mathbf{Mo_2Si_2}$, $\mathbf{Mo_2Si_2^{+\bullet}}$; and $\mathbf{Mo_2Si_2^{2(+\bullet)}}$ computed at the CAM-B3LPY/def2-TZVP with CPCM(DMSO).

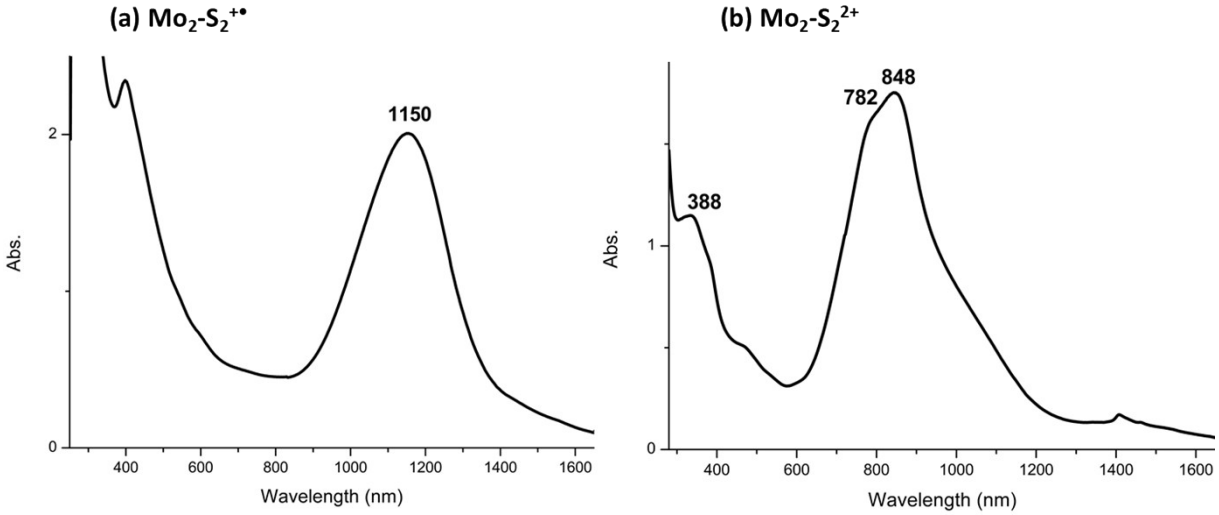

Fig. S7 UV-vis-NIR spectrum of (a) $\mathbf{Mo_2S_2^{+\bullet}}$ in DMSO; (b) $\mathbf{Mo_2S_2^{2+}}$ in MeCN.

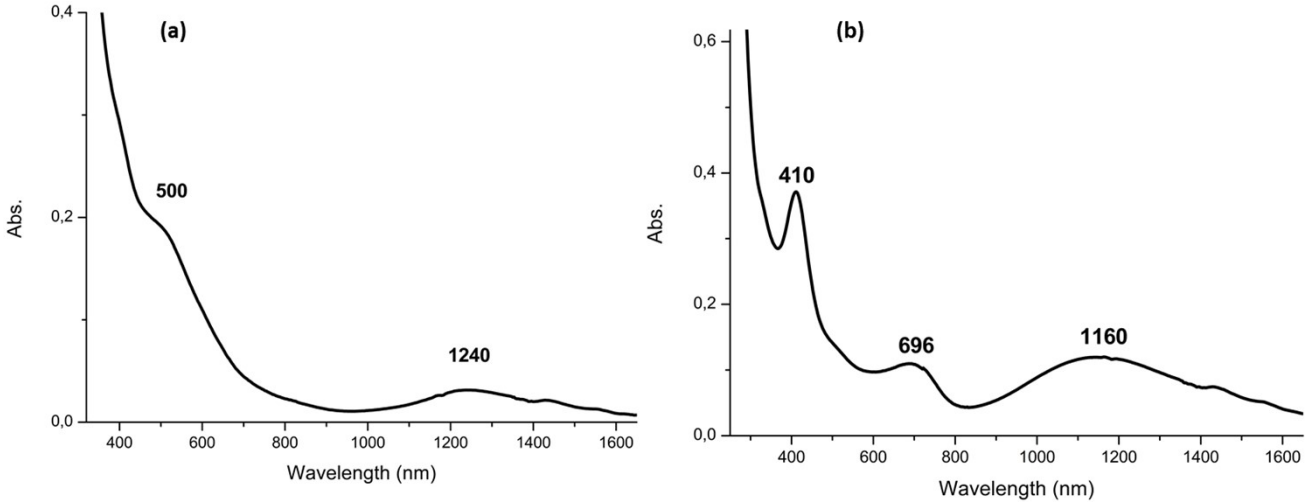

Fig. **S8** UV-vis-NIR spectrum of (a) $\mathbf{Mo_2Si_2}^{+\bullet}$, (b) $\mathbf{Mo_2Si_2}^{2+}$ in DMSO

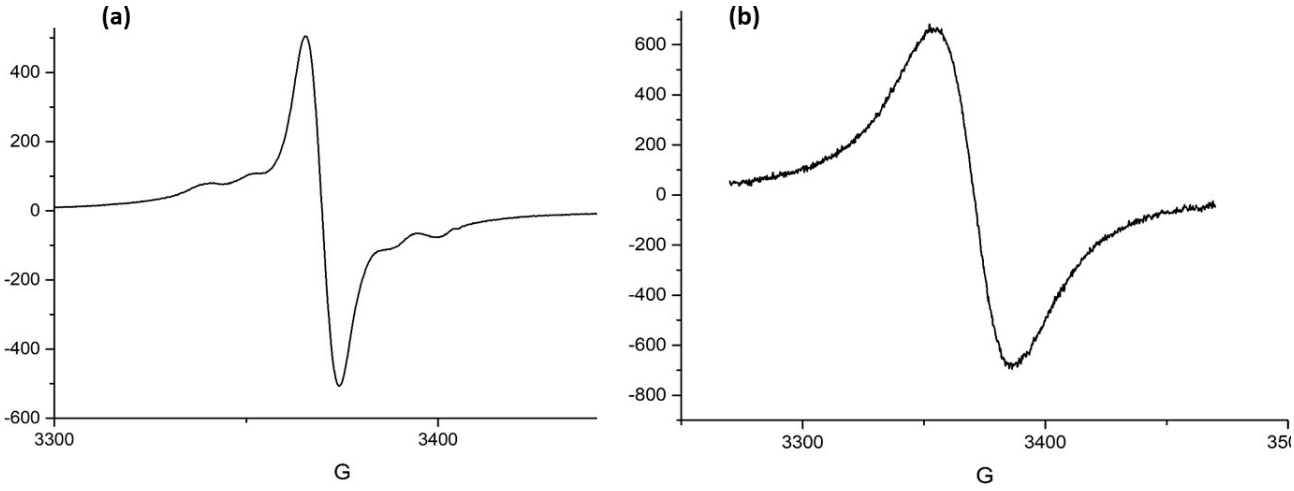

Fig. S9. EPR spectra of $(\mathbf{Mo_2Si_2})(BF_4)_2$ in CH_3CN: (a) at room temperature; (b) frozen solution

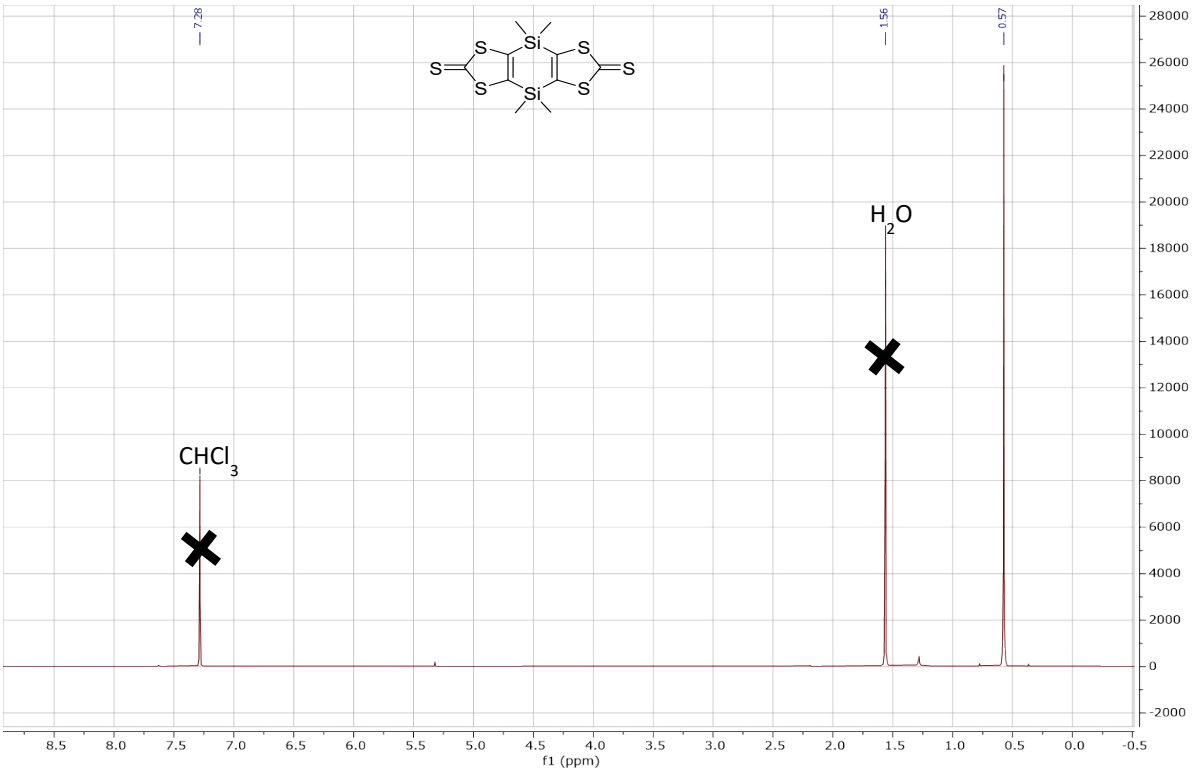

Fig. S10 ^{1}H NMR (300 MHz) of **3** in $CDCl_3$

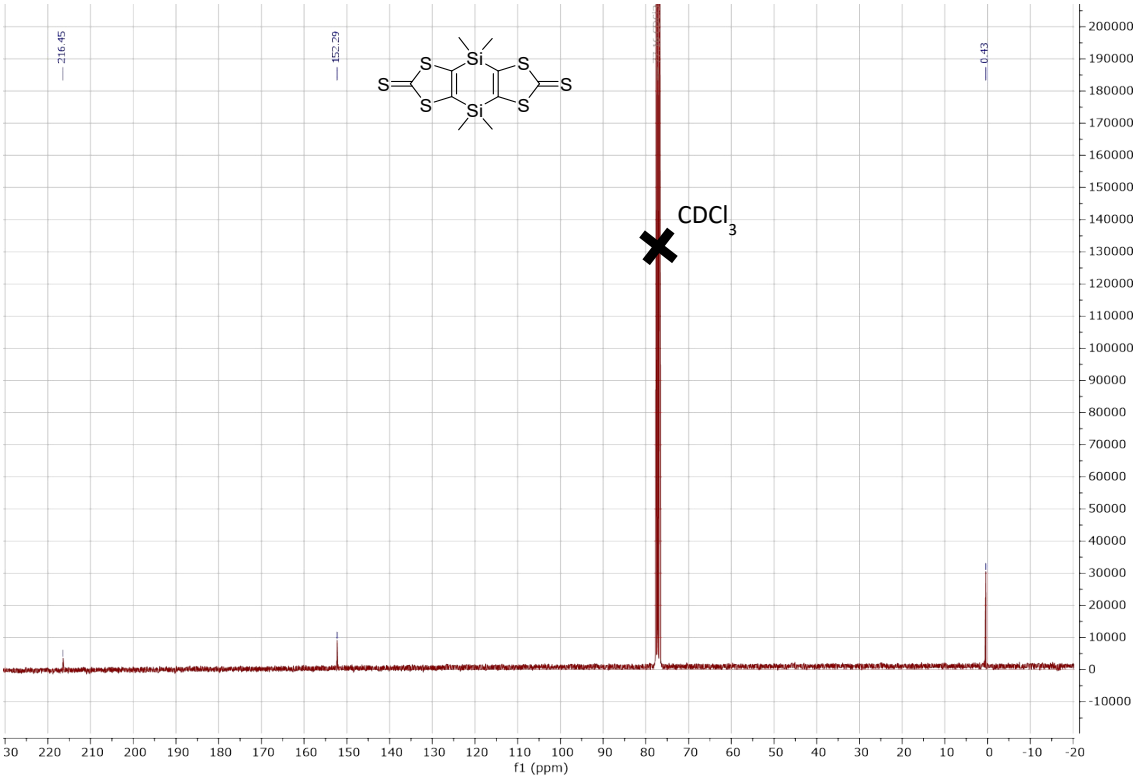

Fig. S11 ^{13}C NMR (75 MHz) of **3** in $CDCl_3$

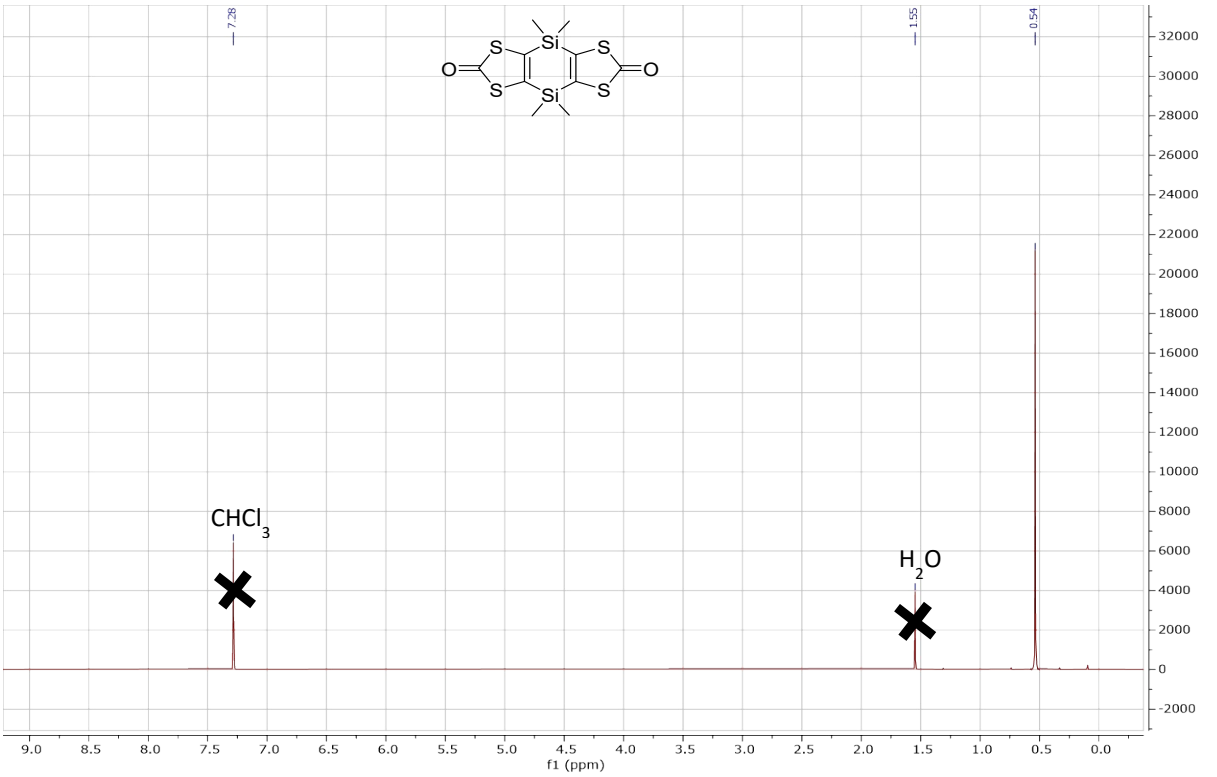

Fig. S12 ^{1}H NMR (300 MHz) of **4** in $CDCl_3$

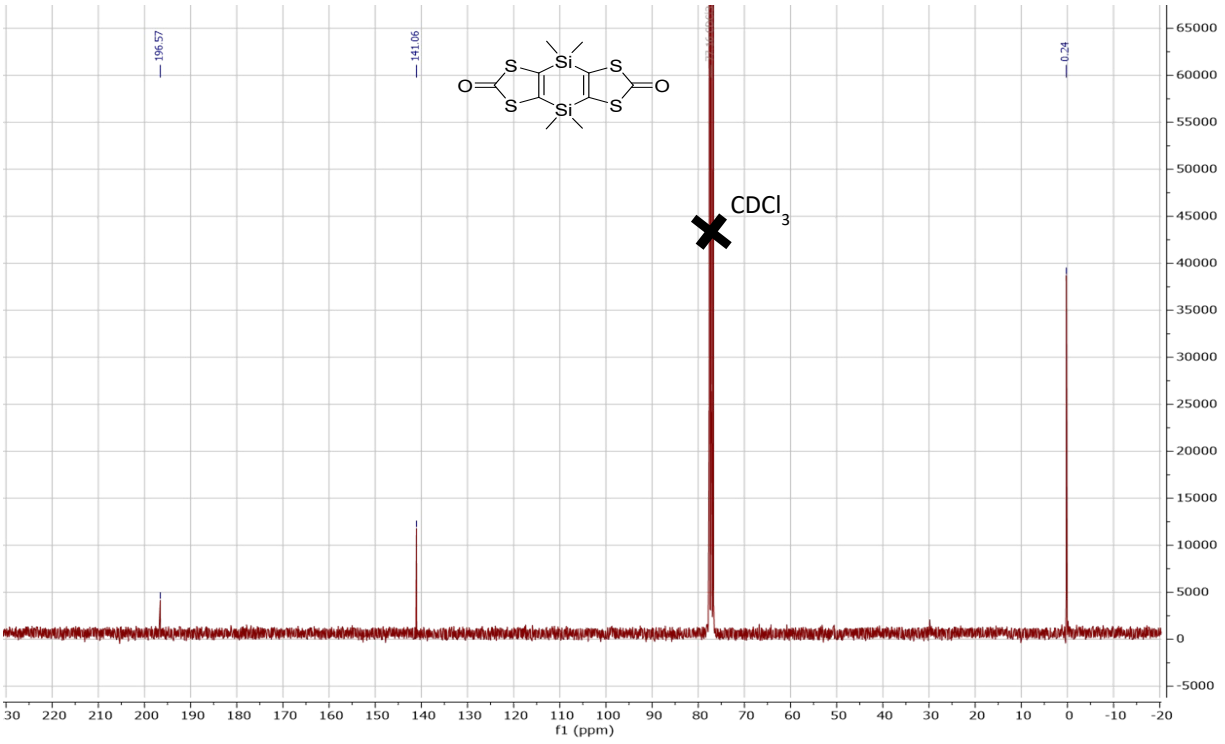

Fig. S13 ^{13}C NMR (75 MHz) of **4** in $CDCl_3$

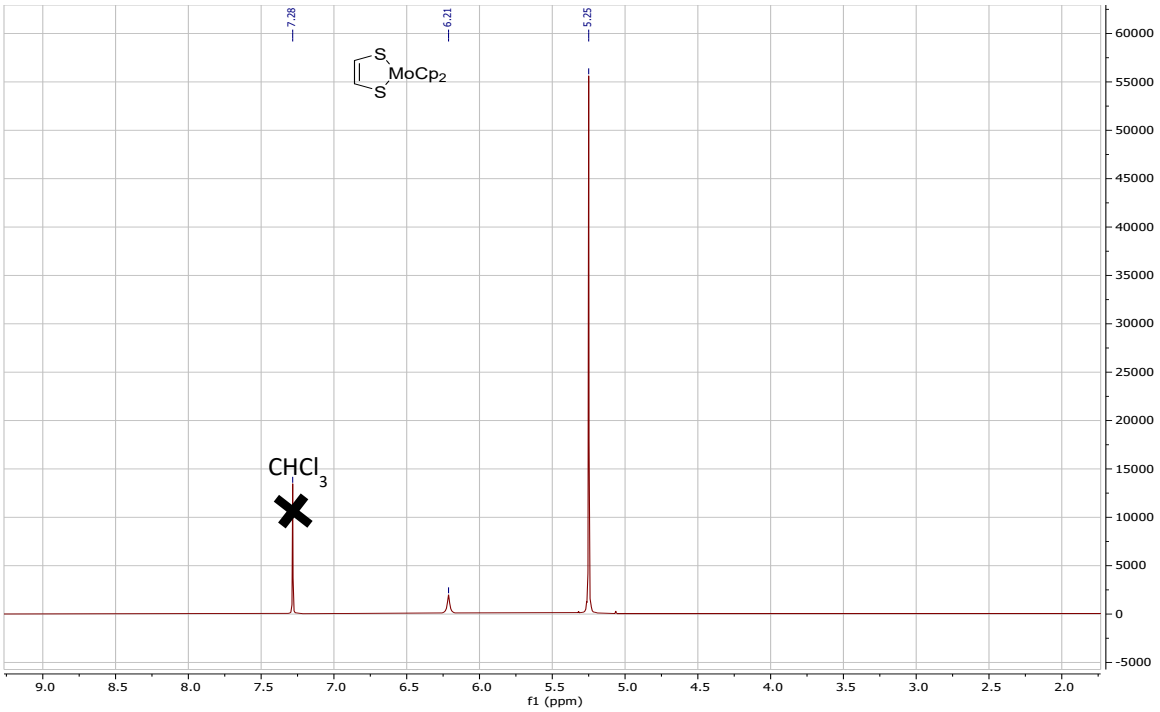

Fig. S14 ^{1}H NMR (300 MHz) of **Modt** in $CDCl_3$

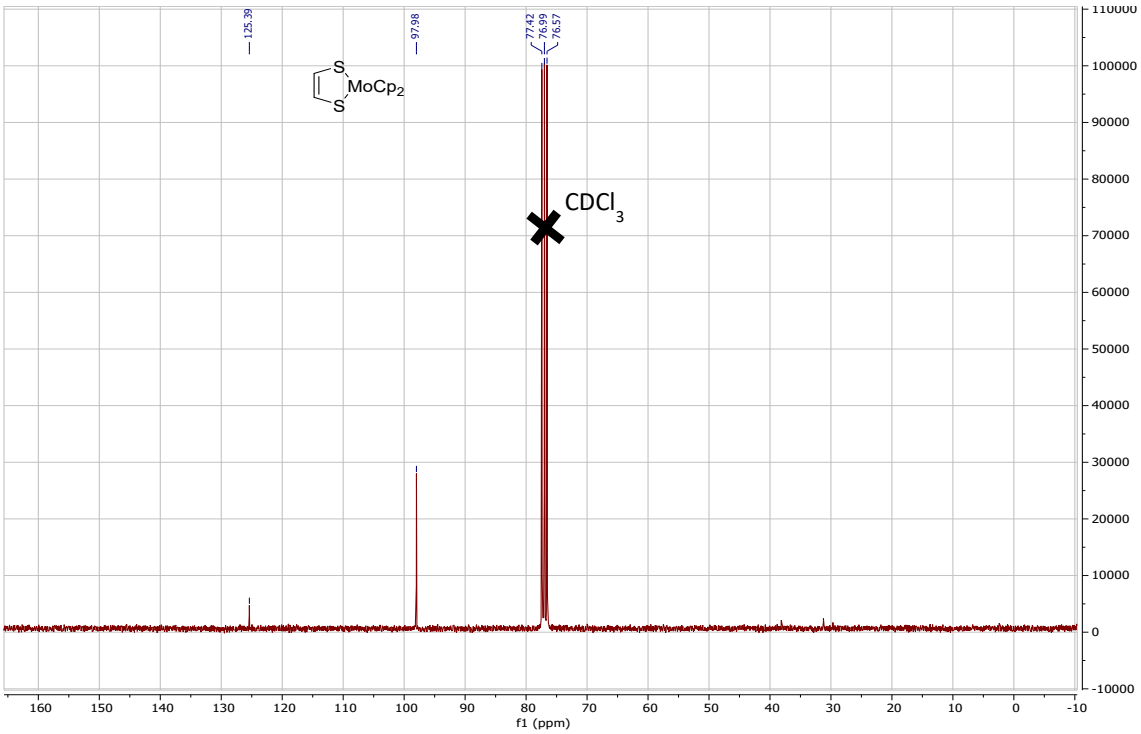

Fig. S15 ^{13}C NMR (75 MHz) of **Modt** in $CDCl_3$

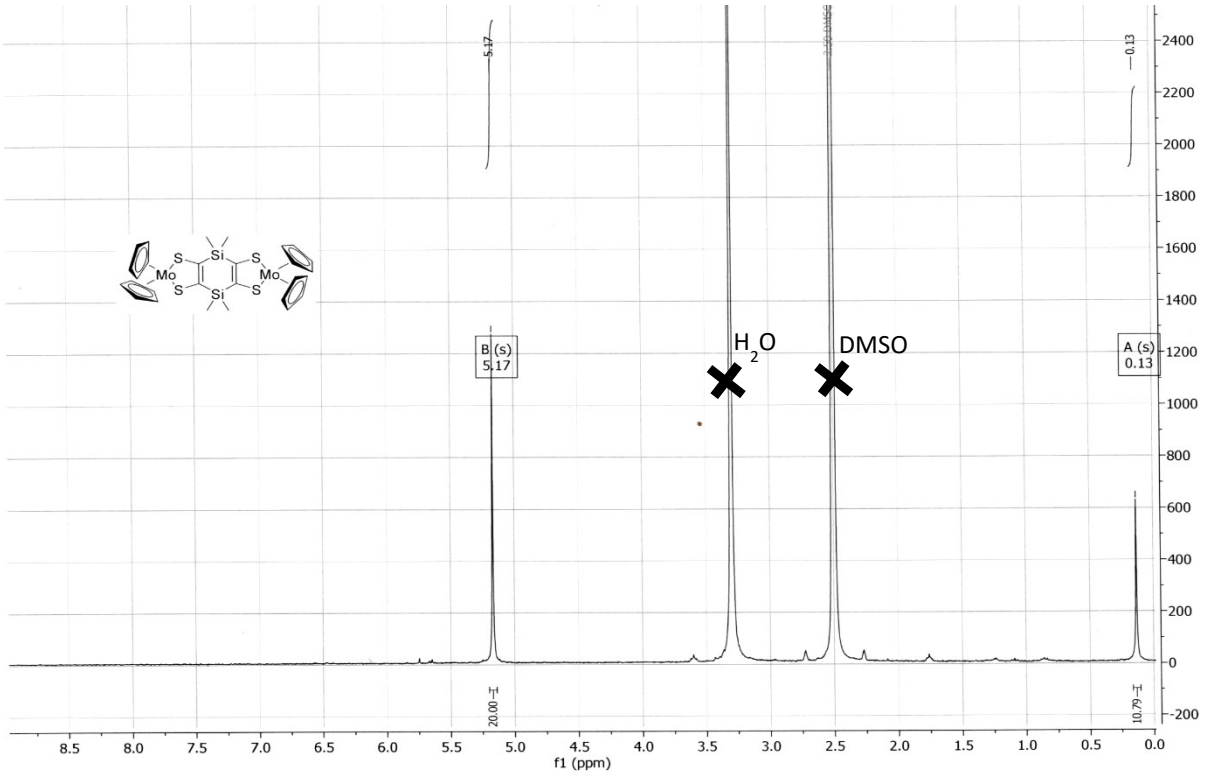

Fig. S16 ^{1}H NMR (400 MHz) of **Mo_2Si_2** in $(CD_3)_2SO$

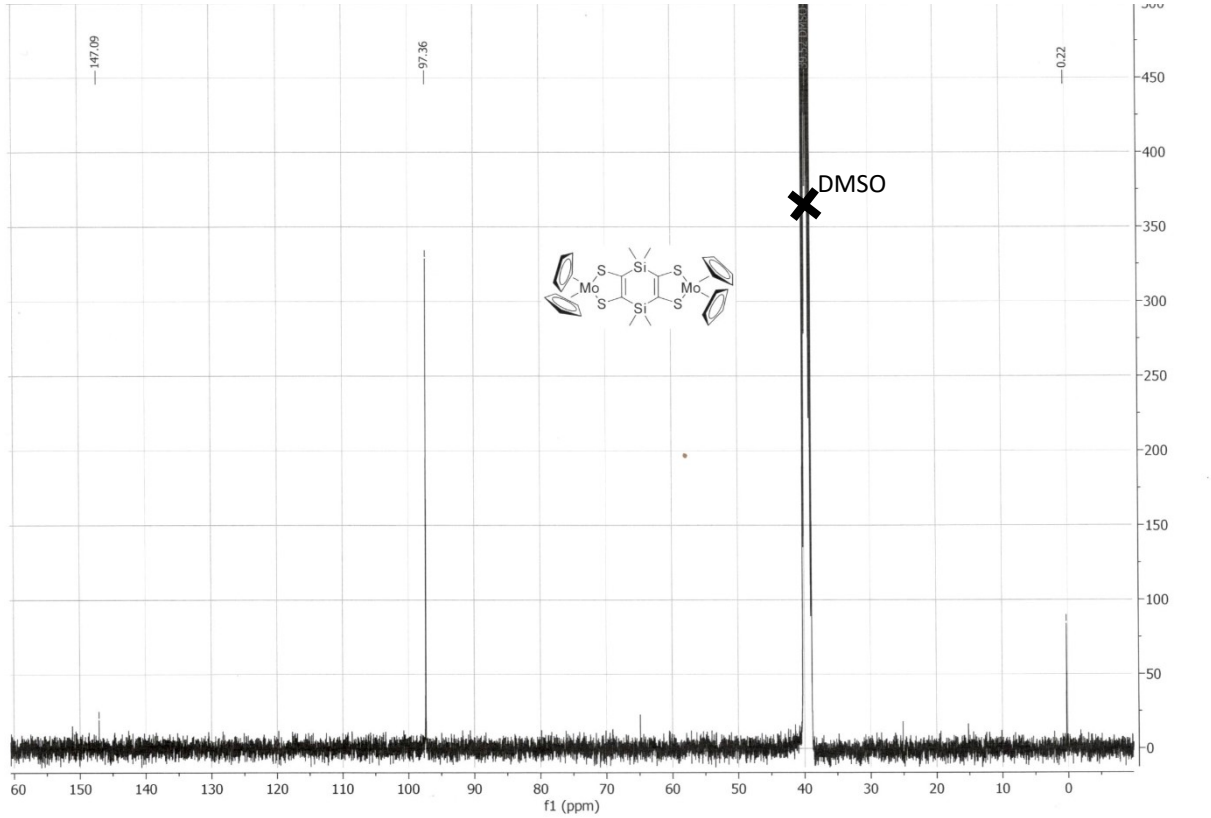

Fig. S17 ^{13}C NMR (101 MHz) of **Mo_2Si_2** in $(CD_3)_2SO$

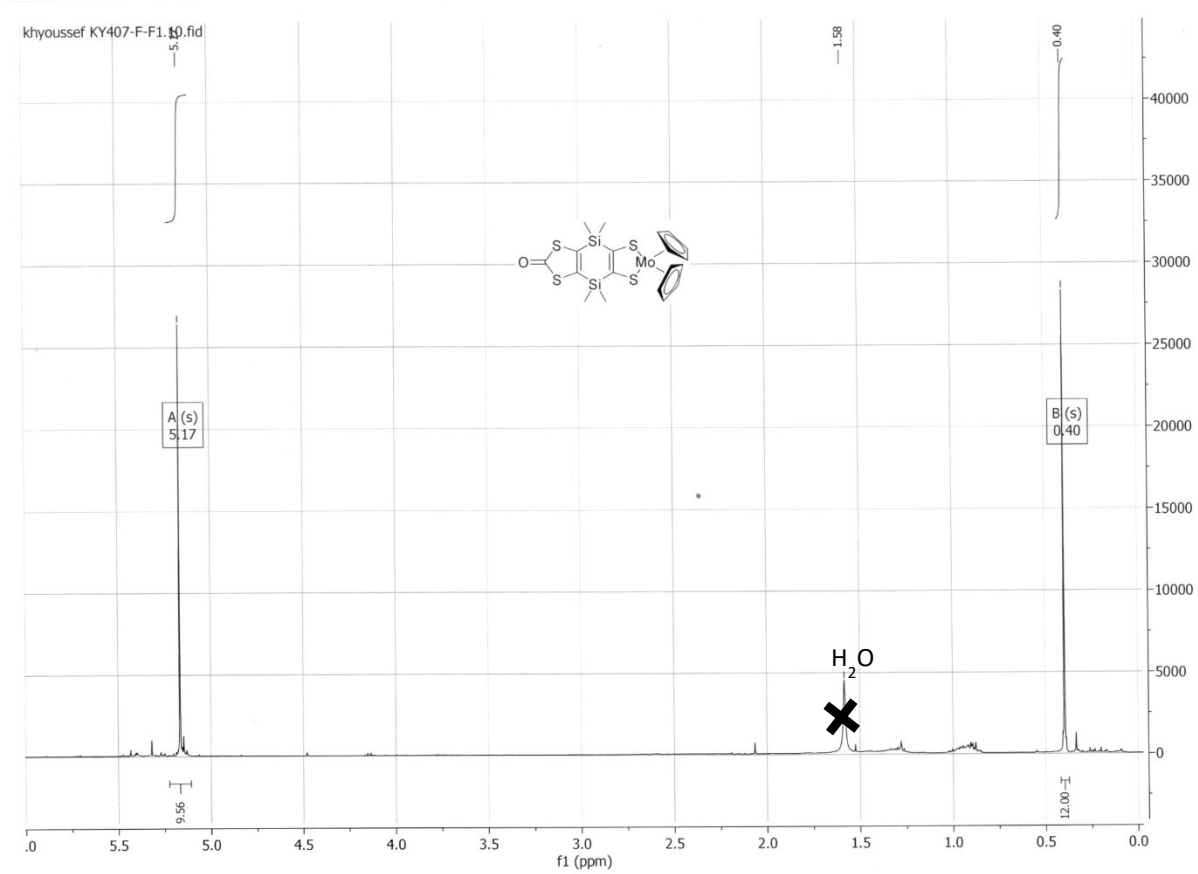

Fig. S18 ^{1}H NMR (400 MHz) of **$MoSi_2$** in $CDCl_3$

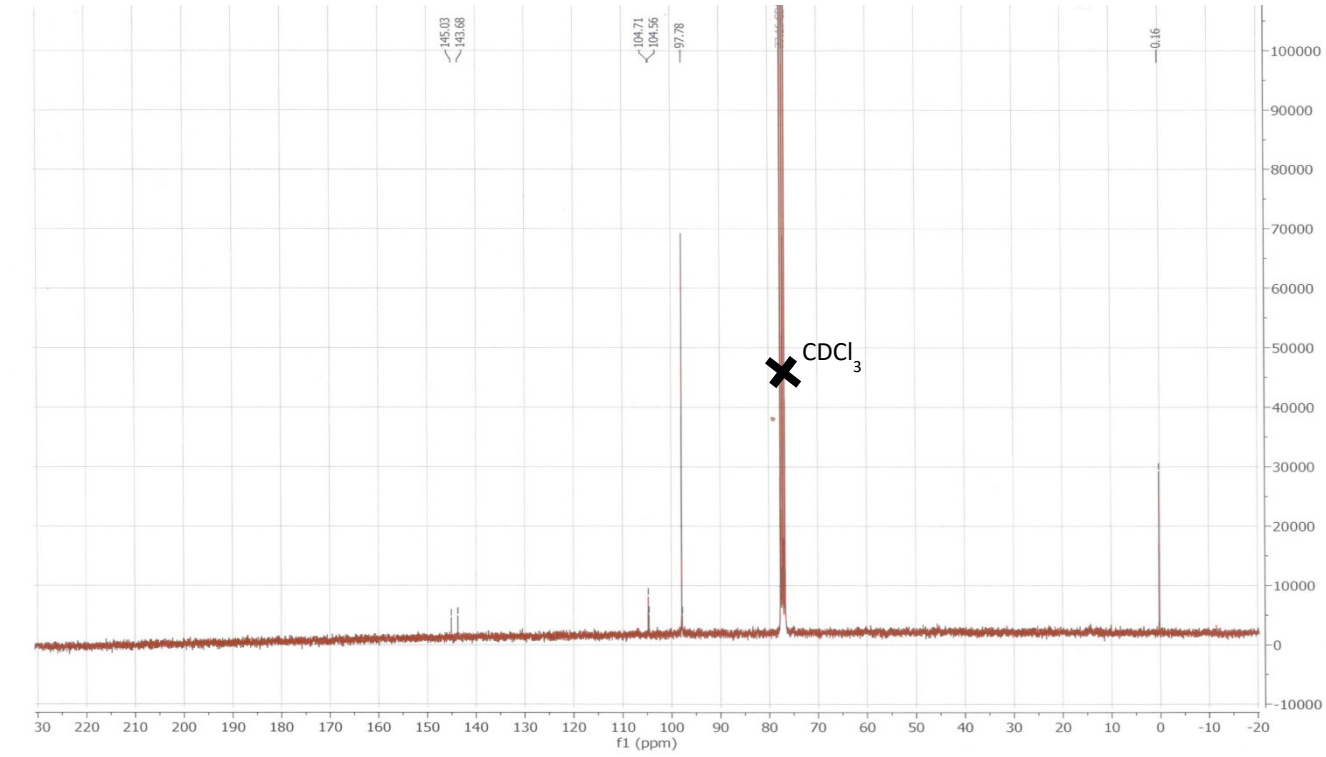

Fig. S19 ^{13}H NMR (75 MHz) of **$MoSi_2$** in $CDCl_3$

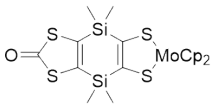

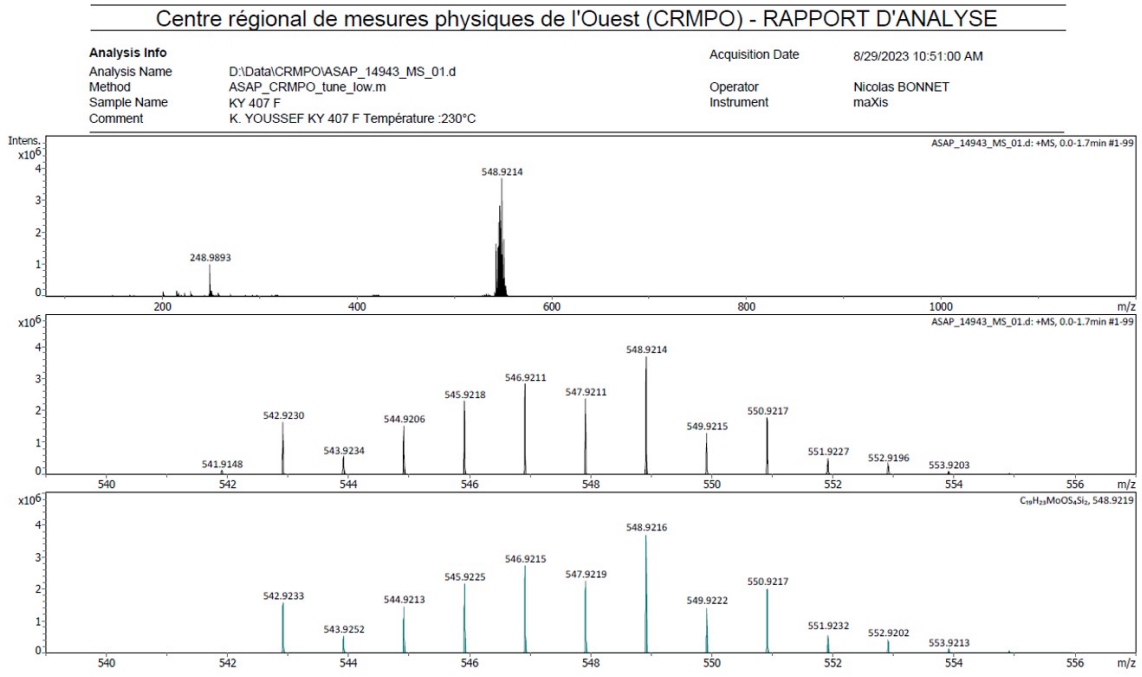

Fig. S20 HRMS of **$MoSi_2$**

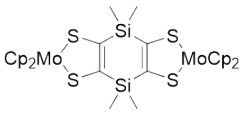

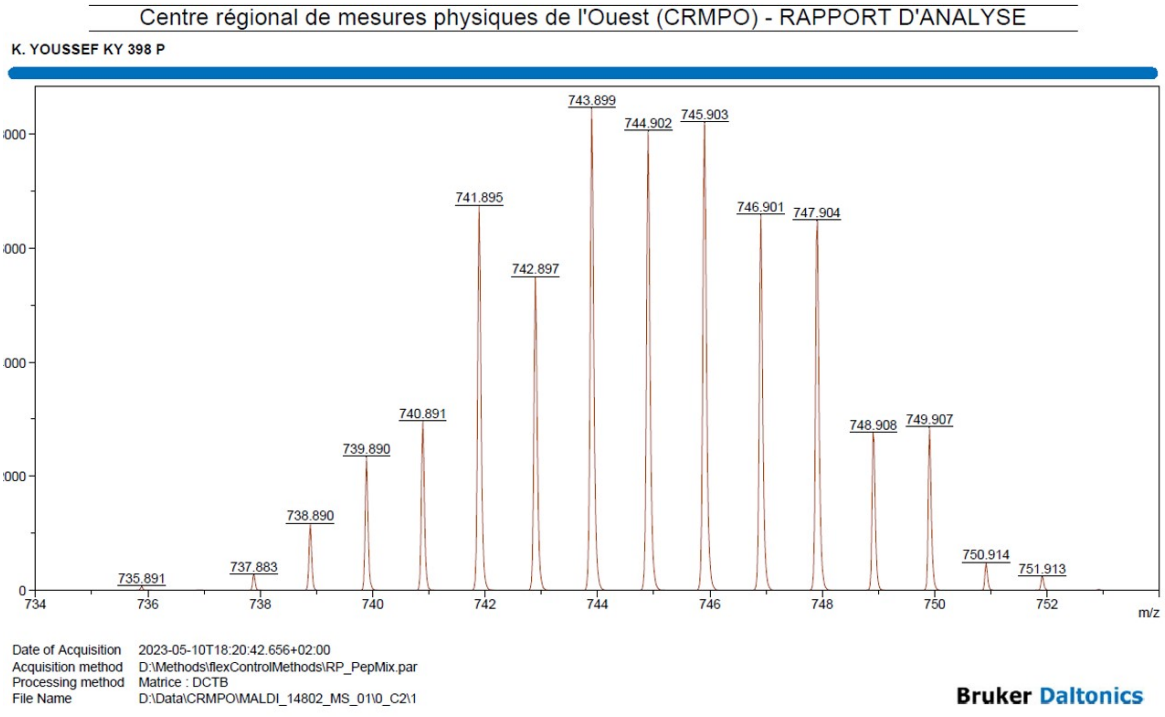

Fig. S21 HRMS of **Mo_2Si_2**

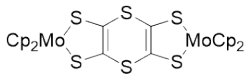

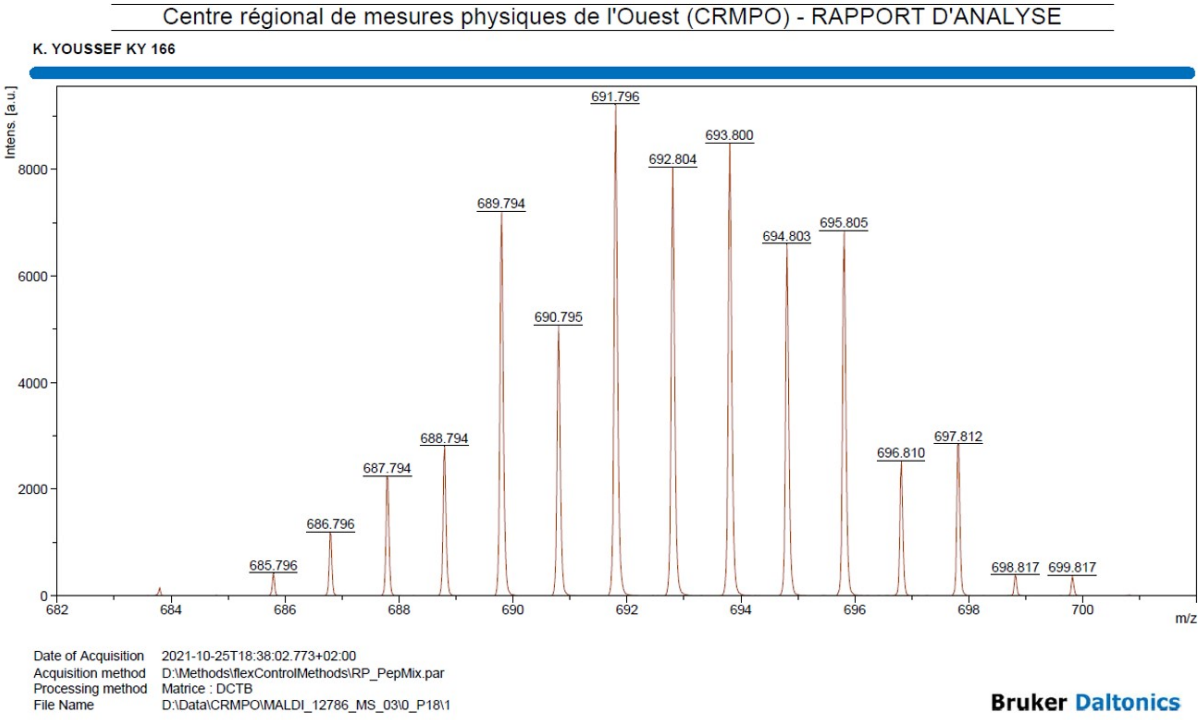

Fig. S22 HRMS of $\mathbf{Mo_2S_2}$

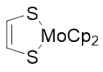

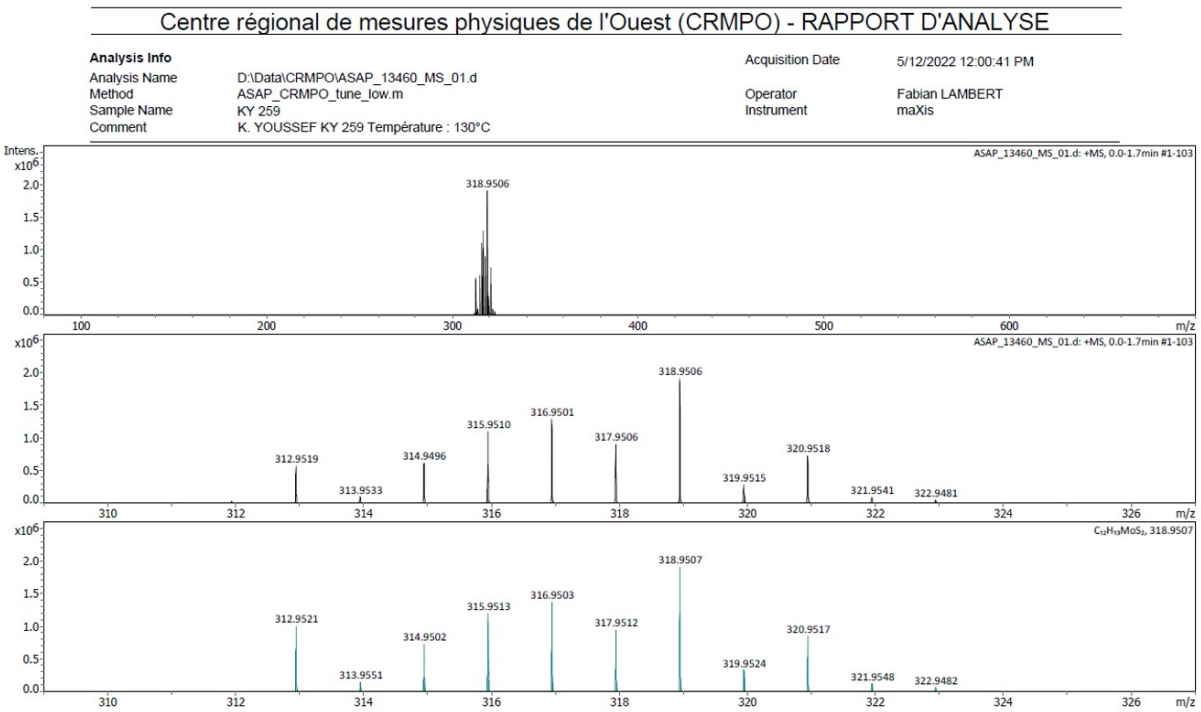

Fig. S23 HRMS of **Modt**